

Theory of integer quantum Hall effect in graphene

Igor F. Herbut

Department of Physics, Simon Fraser University, Burnaby, British Columbia, Canada V5A 1S6

The observed quantization of the Hall conductivity in graphene at high magnetic fields is explained as being due to the dynamically generated spatial modulation of either the electron spin or the density, as decided by the details of Coulomb interaction on the scale of lattice constant. It is predicted that at a large in-plane component of the magnetic field such ordering will be present only at the filling factor $f = \pm 1$, and absent otherwise. Other experimental consequences of the theory are outlined.

Graphene is a two-dimensional semi-metal with gapless Dirac-like excitations near two points in the Brillouin zone [1], [2]. When placed in the uniform magnetic field of several Tesla it exhibits plateaus in the Hall conductivity at integer filling factors $f = 4n + 2$, [3], [4], just as implied by the Landau level (LL) spectrum of the single-particle Dirac equation [5], with each LL being four-fold degenerate in spin and sublattice indices. Although the strength of the Coulomb interaction between the conducting electrons in graphene is similar to the bandwidth, the semi-metallic ground state at zero magnetic field indicates that it is below the critical value needed for insulation [6], [7].

At magnetic fields above $\sim 10T$, however, additional quantum Hall (QH) states at $f = 0, \pm 1, \pm 4$ appear [8]. Plateaus in the Hall conductivity at other integers, such as at $f = \pm 3$ or $f = \pm 5$ for example, are at the same time conspicuously absent, even at the highest magnetic field of $45T$. The experiment [8] also suggests that the activation gaps at $f = \pm 4$ are likely to be due to the Zeeman splitting of the first LL. The quantization at $f = \pm 1$, however, implies that the four-fold degeneracy of the zeroth LL has been completely lifted, which necessitates the inclusion of the Coulomb interactions into consideration. The theory of the integer QH effect in graphene would thus have at least to provide answers to the following questions: a) why has the four-fold degeneracy of *only* the $n = 0$ LL been completely lifted at the magnetic fields and samples under study, b) why do new incompressible states at $f = 0, \pm 1, \pm 4$ require higher magnetic fields to appear than those at $f = 4n + 2$, and finally, c) what is the nature of the interacting ground states at different filling factors.

The first question may be immediately answered by postulating that the Dirac fermions have acquired an effective gap in a form of a ‘relativistic mass’ due to the Coulomb interaction [9]. Such a gap reduces the degeneracy of *only* the zeroth LL. Including the Zeeman splitting then leads to the spectrum of the effective single-particle Hamiltonian precisely as required by the observed pattern of quantization of Hall conductivity. It is unclear, however, under which circumstances, and which one of the multitude of such gaps that could exist, as discussed below, is generated dynamically. This problem is addressed here within the extended Hubbard model on a honeycomb lattice, with both on-site and nearest-

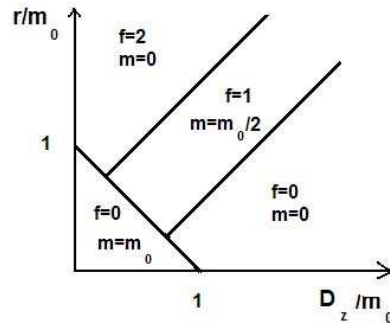


FIG. 1: The proposed phase diagram of graphene in the magnetic field. $D_z = g_z B$ is the Zeeman energy, r the chemical potential, and $m_0 = 2g_x B_{\perp}/\pi$ is the characteristic size of the ‘relativistic’ many-body gap m . g_x is the larger of the couplings in the CDW and AF channels (see the text).

neighbor repulsions. This is the simplest Hamiltonian that mimics the effect of Coulomb repulsion, and which contains the possibilities of charge-density-wave (CDW), and antiferromagnetic (AF) orders. Previous work has shown [7], [10] that these two are in direct competition at zero magnetic field and when the interaction is strong. Here we solve the model in the physical *weak* coupling regime and in an external magnetic field. The results are summarized as the phase diagrams in Figures 1 and 2. At half-filling and for a weak enough Zeeman energy the system could be either a CDW or an AF, depending on which coupling dominates (Fig. 2). For a larger Zeeman energy the ground state at $f = 0$ becomes magnetic with full lattice symmetry. Nevertheless, even in the latter case increasing the chemical potential produces an incompressible state at $f = 1$, with the activation gap becoming equal to the ‘relativistic’ gap (Fig. 1). In contrast, at weak Zeeman coupling we find a direct transition between $f = 0$ and $f = 2$ states. At $f \geq 2$ the ‘relativistic’ gap vanishes. Experiments that would test the presented against other theories [12], [13], [14] are discussed.

We define the extended Hubbard model as $H = H_0 +$

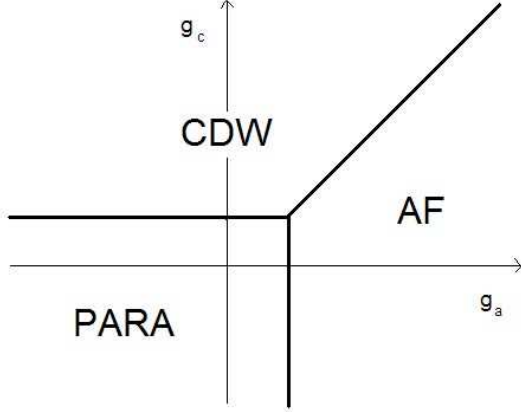


FIG. 2: The phase diagram at half-filling ($r = 0$). The translationally symmetric magnet exists for $g_c, g_a < \pi g_z B / 2B_\perp$.

H_1 , where

$$H_0 = -t \sum_{\vec{A}, i, \sigma=\pm} u_\sigma^\dagger(\vec{A}) v_\sigma(\vec{A} + \vec{b}_i) + H.c., \quad (1)$$

$$H_1 = U \sum_{\vec{X}} n_+(\vec{X}) n_-(\vec{X}) + \frac{V}{2} \sum_{\vec{A}, i, \sigma, \sigma'} n_\sigma(\vec{A}) n_{\sigma'}(\vec{A} + \vec{b}_i). \quad (2)$$

The sites \vec{A} denote one triangular sublattice of the honeycomb lattice, generated by linear combinations of the basis vectors $\vec{a}_1 = (\sqrt{3}, -1)(a/2)$, $\vec{a}_2 = (0, a)$. The second sublattice is then at $\vec{B} = \vec{A} + \vec{b}$, with the vector \vec{b} being either $\vec{b}_1 = (1/\sqrt{3}, 1)(a/2)$, $\vec{b}_2 = (1/\sqrt{3}, -1)(a/2)$, or $\vec{b}_3 = (-a/\sqrt{3}, 0)$. $a \approx 2.5A$ is the lattice spacing, and $t \approx 2.5\text{eV}$, $U \approx 5 - 12\text{eV}$, and $U/V \approx 2 - 3$ [10].

The spectrum of H_0 becomes linear in the vicinity of the two Dirac points at $\pm \vec{K}$, with $\vec{K} = (1, 1/\sqrt{3})(2\pi/a\sqrt{3})$ [1], [2]. Retaining only the Fourier components near $\pm \vec{K}$ one can write, in the continuum notation,

$$H_0 = \int d\vec{x} \sum_\sigma \Psi_\sigma^\dagger(\vec{x}) i\gamma_0 \gamma_i D_i \Psi_\sigma(\vec{x}), \quad (3)$$

and

$$\Psi_\sigma^\dagger(\vec{x}) = \int^\Lambda \frac{d\vec{q}}{(2\pi a)^2} e^{-i\vec{q}\cdot\vec{x}} (u_\sigma^\dagger(\vec{K} + \vec{q}), v_\sigma^\dagger(\vec{K} + \vec{q}), u_\sigma^\dagger(-\vec{K} + \vec{q}), v_\sigma^\dagger(-\vec{K} + \vec{q})), \quad (4)$$

$i = 1, 2$, where it was convenient to rotate the reference frame so that $q_1 = \vec{q} \cdot \vec{K}/K$ and $q_2 = (\vec{K} \times \vec{q}) \times \vec{K}/K^2$, and set $\hbar = e/c = v_F = 1$, where $v_F = ta\sqrt{3}/2$ is the Fermi velocity. Here $i\gamma_0\gamma_1 = \sigma_z \otimes \sigma_x$, $i\gamma_0\gamma_2 = -I_2 \otimes \sigma_y$, with I_2 as the 2×2 unit matrix, and $\vec{\sigma}$ as the Pauli matrices. $\Lambda \approx 1/a$ is the ultraviolet cutoff over which

the linear approximation for the dispersion holds. The orbital effect of the magnetic field is included by defining $D_i = -i\partial_i - A_i$, with its component perpendicular to the graphene's plane being $B_\perp = \partial_1 A_2 - \partial_2 A_1$.

Consider an auxiliary single-particle Hamiltonian \tilde{H} :

$$\tilde{H} = mM + i\gamma_0\gamma_i D_i, \quad (5)$$

where M is a Hermitean 4×4 matrix. When $m = 0$, $\tilde{H} = H_0$, for each spin state. Also, if $M^2 - 1 = \{M, \gamma_0\gamma_i\} = 0$,

$$\tilde{H}^2 = D_i^2 + B(\sigma_z \otimes \sigma_z) + m^2. \quad (6)$$

This is the case if, either

$$M = M_1 = a(I_2 \otimes \sigma_z) + b(\sigma_x \otimes \sigma_x) + c(\sigma_y \otimes \sigma_x) \quad (7)$$

with real a, b, c that satisfy $a^2 + b^2 + c^2 = 1$, or

$$M = M_2 = \sigma_z \otimes \sigma_z. \quad (8)$$

In either case the eigenvalues of \tilde{H}^2 are at $nB + m^2$, with $n = 0, 1, 2, \dots$. For $n > 0$ this immediately implies that eigenvalues of \tilde{H} itself are at $\pm\sqrt{nB + m^2}$, with the degeneracies of B/π per unit area being the same as for $m = 0$. For $n = 0$, on the other hand, an elementary calculation gives that the eigenvalues of \tilde{H} , a) for any M_1 , are at $\pm|m|$, each with halved degeneracy of $B/2\pi$ (per unit area), and, b) for M_2 , are at m , still with the degeneracy of B/π . The invariance of the spectrum in the first case under rotations of the unit vector (a, b, c) is the consequence of the ‘chiral’ $SU(2)$ symmetry of H_0 generated by $\{\gamma_{35}, \gamma_3, \gamma_5\}$, where $\gamma_3 = \sigma_x \otimes \sigma_y$, $\gamma_5 = \sigma_y \otimes \sigma_y$, and $\gamma_{35} = i\gamma_3\gamma_5$, for example [7], [11]. Any specific choice of M_1 in \tilde{H} breaks this $SU(2)$ down to $U(1)$, and leads to the same eigenvalues. M_2 preserves the chiral symmetry, and hence implies a different spectrum.

Assuming that such an effective chiral-symmetry-breaking gap m becomes generated by interactions and then splitting the resulting energy levels by the Zeeman effect could thus lead to the QH states at all even f , $f = 0$, and $f = \pm 1$, in accord with experiment [8]. This still, however, leaves a complete freedom of choice of the vector (a, b, c) . In particular, this choice may differ for the two spin states as well. For example, at $B = 0$ and at strong V , one expects the interactions to prefer $a = 1$ for both projections of spin, i. e. the CDW [2]. For strong U and at $B = 0$, on the other hand, it is $a = \sigma$, i. e. the AF, that has lower energy [7]. $a = 0$ would correspond to the competing ‘Kekule’ ordering [15]. Which direction on chiral manifold is actually chosen by the system is thus obviously a question of dynamics, to which we turn next.

The low energy Lagrangian for the extended Hubbard model may be written as [7]

$$L = i \sum_\sigma \bar{\Psi}_\sigma \gamma_\mu D_\mu \Psi_\sigma - \sum_\sigma (r + \sigma g_z B) \bar{\Psi}_\sigma \Psi_\sigma \quad (9)$$

$$- g_c (\sum_\sigma \bar{\Psi}_\sigma \Psi_\sigma)^2 - g_a (\sum_\sigma \sigma \bar{\Psi}_\sigma \Psi_\sigma)^2,$$

where $\bar{\Psi}_\sigma = \Psi_\sigma^\dagger(\vec{x}, \tau)\gamma_0$, $D_0 = -i\partial_\tau$, with τ as the imaginary time, $\mu = 0, 1, 2$, and $\gamma_0 = I_2 \otimes \sigma_z$, $\gamma_1 = \sigma_z \otimes \sigma_y$, and $\gamma_2 = I_2 \otimes \sigma_x$. Here $g_a \approx Ua^2/8$, $g_c \approx (3V - U)a^2/8$, g_z is the effective g -factor of the electron, and $B = (B_\perp^2 + B_\parallel^2)^{1/2}$, with B_\parallel as the field's in-plane component. We have retained only the *two least irrelevant* short-range interactions among those present in the full effective Lagrangian at $B = 0$ [7]. This will prove justified at the magnetic fields of interest, as discussed shortly.

Performing the Hubbard-Stratonovich transformation and neglecting the quantum fluctuations the free energy per unit area and at $T = 0$ may be written as

$$F(m_c, m_a) - F(0, 0) = \frac{m_c^2}{4g_c} + \frac{m_a^2}{4g_a} + \frac{B_\perp}{4\pi^{3/2}} \int_0^\infty \frac{ds}{s^{3/2}} \sum_{\sigma=\pm} (e^{-sm_\sigma^2} - 1) f_\sigma(s, m_\sigma), \quad (10)$$

where $m_\sigma = m_c + \sigma m_a$, and the function

$$f_\sigma(s, m) = \theta(|m| - |r + \sigma g_z B|) + C(s\Lambda^2) (\coth(\frac{sB_\perp}{2}) - 1). \quad (11)$$

$m_c/g_c = \sum_\sigma \langle \bar{\Psi}_\sigma \Psi_\sigma \rangle$, $m_a/g_a = \sum_\sigma \sigma \langle \bar{\Psi}_\sigma \Psi_\sigma \rangle$, are the CDW and the AF order parameters [7], respectively. $C(x)$ is the cutoff function that satisfies $C(x \rightarrow \infty) = 1$ and $C(x \rightarrow 0) = 0$. Summing over the LLs below a sharp cutoff in energy, for example, yields $C(x) = 1 - e^{-x}$. The first term in Eq. (11) represents the crucial zeroth LL contribution, and the second the remaining LLs. Zeeman energy is taken to always be smaller than the separation between the LLs, i. e. $g_z B < \sqrt{B_\perp}$.

Let us first consider the system at $r = 0$. The free energy is minimized by the solution of

$$\frac{m_+}{g_+} + \frac{m_-}{g_-} = \frac{4B_\perp}{\pi^{3/2}} \int_0^\infty \frac{ds}{s^{1/2}} e^{-s} f_+(\frac{s}{m_+^2}, m_+), \quad (12)$$

$$\frac{m_-}{g_+} + \frac{m_+}{g_-} = \frac{4B_\perp}{\pi^{3/2}} \int_0^\infty \frac{ds}{s^{1/2}} e^{-s} f_-(\frac{s}{m_-^2}, m_-), \quad (13)$$

where $g_\pm^{-1} = g_c^{-1} \pm g_a^{-1}$. Assume that both g_c and g_a to be weak and positive, and that $g_c > g_a$, for example. There are then three types of solutions:

1) If $m_+ \geq m_- > g_z B$, then $m_+ = m_-$, i. e. $m_a = 0$ and $m_c = 2g_c B_\perp/\pi$. This is the CDW. It exists when $g_c > \pi g_z B/2B_\perp$. For $g_a > g_c$, of course, one finds $m_c = 0$ and $m_a = 2g_a B_\perp/\pi$, i. e. the AF (Fig. 2). This, in particular, includes the case of the pure Hubbard model with $V = 0$. The linear dependence on B_\perp reflects the proportionality of either m to the degeneracy of the LLs.

2) For $g_z B > m_+ \geq m_-$ one finds a paramagnet with $m_c = m_a = 0$, unless the stronger coupling exceeds the $B = 0$ critical value of $\pi/8\Lambda$.

3) Finally, when $m_+ > g_z B > |m_-|$, the solution is $m_x = g_x B_\perp/\pi$, where $x = c, a$. Both the CDW

and the AF order parameters are finite, which would corresponds to a *ferrimagnet*. This solution exists for $g_c + g_a > \pi g_z B/B_\perp$, and $|g_c - g_a| < \pi g_z B/B_\perp$.

At weak coupling only the first term, representing the zeroth LL in Eq. (11), actually matters for the gap m . The second term becomes important only at strong couplings, or when $B_\perp \rightarrow 0$. Comparing the energies of the four possible solutions, we find only three stable phases, depicted in Fig. 2. All three have the filling factor $f = 0$. Even if both g_c and g_a are positive it is always energetically favorable to open a single but bigger gap that corresponds to the dominant coupling. The aforementioned ferrimagnet, which would have $f = 1$, is thus never the minimum of the energy at $r = 0$. This may also be understood as follows. At low magnetic fields, such that $l_B \gg a$ where $l_B = 1/\sqrt{B_\perp}$ is the magnetic length, the flow of the couplings implied by the invariance of the gaps in Eqs. (12)-(13) with respect to change of the cutoff Λ is the same as at $B_\perp = 0$. All weak couplings are thus infrared irrelevant in this regime [7]. At $B_\perp \neq 0$ the flow of the interaction couplings towards the stable Gaussian fixed point is terminated at the cutoff $\sim 1/l_B$, with the least irrelevant coupling being left as dominant in the low energy theory. This single coupling then selects and generates the ‘relativistic’ gap at $B_\perp \neq 0$. All other more irrelevant couplings can be neglected, as we partially did in Eq. (9), from the outset. Incidentally, this also justifies the Hartree approximation to the free energy in Eq. (10): as long as the ground state is semi-metallic and gapless at $B_\perp = 0$, for a weak enough magnetic field the low energy theory below the cutoff $\sim 1/l_B \ll 1/a$ is indeed weakly interacting, as assumed.

It is useful to display the relevant energy scales in the problem. First, the ‘relativistic’ gap is $m \approx (U/8)(B_\perp/B_0)$, where $B_0 = 1/a^2 \approx 10^5 T$ is the characteristic scale for the magnetic field set by the lattice constant. Assuming $U \approx 10\text{eV}$ gives $m \approx 1\text{meV}$ for $B_\perp \sim 10T$. The LL separation, on the other hand, is $D_L \approx t(B_\perp/B_0)^{1/2}$, and thus by roughly two orders of magnitude larger. The Zeeman energy, on the other hand, for $g_z \approx 1$ is $D_z \approx (B/10^4 T)\text{eV}$, and thus of a similar size as m . Since the widths of the plateaus at $f = 0, \pm 1, \pm 4$ are proportional to m or D_z , both much smaller than D_L , this would naturally explain why these QH states require higher magnetic fields to become discernible.

At $r = 0$ there are thus two fundamentally different ground states: one at larger interactions that breaks the $A - B$ sublattice symmetry, either in the charge (CDW) or the spin (AF) channel, with vanishing magnetization, and the other, magnetic, at weaker interactions, with the full translational symmetry of the lattice. Both are incompressible, and yield the plateau in the Hall conductivity at $f = 0$. If the parameters are such to place the system for $B_\parallel = 0$ into the former, increasing B_\parallel would eventually cause the transition into the latter state.

Hereafter we retain only the larger quartic coupling and its corresponding order parameter in Eq. (10). The

search for minima of the free energy then leads to the phase diagram at a finite chemical potential presented in Fig. 1. For $f \geq 2$ the ‘relativistic’ gap is $m = 0$, and there is a direct transition between $f = 0$ to $f = 2$ at $D_z/m_0 < 1/4$. For a fixed and larger D_z , by increasing the chemical potential the system always passes through the intermediate $f = 1$ QH state, which is magnetic and breaks the discrete sublattice symmetry. The width of $f = 1$ state is $2D_z - (m_0/2)$ for $D_z/m_0 < 3/4$, or m_0 for $D_z/m_0 > 3/4$. All transitions are discontinuous. As the ratio D_z/m_0 can be changed by varying B_{\parallel} , it follows that at a large enough B_{\parallel} the width and the activation energy of the $f = \pm 1$ state becomes $\sim B_{\perp}$ and independent of B_{\parallel} , which should be experimentally testable. Since in the experiment [8] the width of the plateau at $f = 0$ appears to be somewhat larger than at $f = \pm 1$ and $f = \pm 4$, the latter being always $2D_z$, we speculate that $1/4 < D_z/m_0 < 1/2$. If this is indeed the case the activation energy at $f = 0$ should first decrease before increasing with B_{\parallel} , whereas that of $f = 1$ would increase and saturate.

The mechanism of ‘magnetic catalysis’ of the ‘relativistic’ gap [9] utilized here has also been considered as an explanation of the integer QH effect in graphene in ref. [12]. The crucial difference from the present work is that only $\sim 1/r$ tail of the Coulomb interaction was included, which could produce only the CDW, and that with the large gap $m \sim \sqrt{B_{\perp}} \sim D_L$. To have m much smaller from the LL separation, as observed, requires then what appears to be an unrealistically strong screening of the Coulomb interaction by the substrate [12]. In this theory the gap is also always inhibited by a finite chemical potential, and thus cannot exist at $f = 1$ if it did not already at $f = 0$. This would imply that the activation gap in [12] at $f = 1$ is always the Zeeman energy. Both results are in sharp contradiction with ours.

The QH effect in graphene was also recently discussed in [13]. The principal difference from the present work is

that the AF ordering was entirely neglected, so that the existence of the QH state at $f = 1$ in [13] is always due to the CDW, which then requires a large enough V . In contrast, in the present theory $f = 1$ state can exist even for $V = 0$, when it is due to the AF ordering. In particular, setting $V = g_z = 0$ we find the pure ($V = 0$) weakly coupled Hubbard model at half filling and in magnetic field to be an AF, and not the Stoner’s ferromagnet, as assumed in [13]. This is because a finite AF order parameter, unlike the magnetization, besides splitting the zeroth LL, also lowers the energy of all other occupied LLs. Put differently, in considering the dynamics within only the zeroth LL, the couplings need to be renormalized up to the length scale of the magnetic length l_B first. Then $g_a(l_B) \gg g_f(l_B)$ always, where g_f is the coupling in the ferromagnetic channel [7], for this reason omitted in Eq. (9). Retaining such a ferromagnetic coupling may be shown to only increase the activation energy when $m = 0$ to $D_z + 2g_f B_{\perp}/\pi$.

Finally, the present mechanism differs essentially from the recent proposal [14], in which disorder is invoked to explain the absence of QH states at odd $f \neq \pm 1$.

To summarize, we assumed that the main effect of Coulomb interaction in graphene is to introduce the on-site and nearest-neighbor repulsion for electrons on a honeycomb lattice. Postulating further a semi-metallic ground state in zero field, the phase diagram of graphene at laboratory magnetic fields $\sim 10T$ is proposed. The theory predicts the incompressible states at all even integer filling factors including $f = 0$, and at $f = \pm 1$. The ground state of the system at $f = 0$ either breaks the sublattice symmetry, in either charge or spin channels, or it is magnetic, depending on the magnitude of the Zeeman energy. At $f = \pm 1$ the system is always in the translational symmetry breaking phase and with finite magnetization, whereas at $|f| \geq 2$ the sublattice symmetry is preserved.

This work was supported by the NSERC of Canada.

[1] P. K. Wallace, Phys. Rev. **71**, 622 (1947).
[2] G. W. Semenoff, Phys. Rev. Lett. **53**, 2449 (1984).
[3] K. S. Novoselov et. al., Nature **438**, 197 (2005).
[4] Y. Zhang et. al., Nature **438**, 201 (2005).
[5] V. P. Gusynin and S. G. Sharapov, Phys. Rev. Lett. **95**, 146801 (2005); N. M. R. Peres, F. Guinea, and A. H. Castro Neto, Phys. Rev. B **72**, 174406 (2005).
[6] D. V. Khveshchenko, Phys. Rev. Lett. **87**, 246802 (2001).
[7] I. F. Herbut, Phys. Rev. Lett. **97**, 146401 (2006).
[8] Y. Zhang et. al., Phys. Rev. Lett. **96**, 136806 (2006).
[9] V. P. Gusynin, V. A. Miransky, and I. A. Shovkovy, Phys. Rev. Lett. **73**, 3499 (1994).
[10] A. L. Tchougueff and R. Hoffmann, J. Phys. Chem. **96**, 8993 (1992).
[11] See also, I. F. Herbut, Phys. Rev. Lett. **88**, 047006 (2002); Phys. Rev. B **66**, 094504 (2002), for analogous chiral symmetry of d-wave superconductors.
[12] V. P. Gusynin et al., preprint cond-mat/0605348.
[13] J. Alicea and M. P. A. Fisher, Phys Rev. B **74**, 075422 (2006).
[14] K. Nomura, and A. H. MacDonald, Phys. Rev. Lett. **96**, 256602 (2006).
[15] C-Y. Hou, C. Chamon, and C. Mudry, preprint cond-mat/0609740.